Predicting the Thermodynamic Stability of Zirconium Radiotracers

Holland, Jason P

Abstract: The thermodynamic stability of a metal−ligand complex, as measured by the formation constant (log), is one of themost important parameters that determines metal ion selectivity and potential applications in, for example, radiopharmaceuticalscience. The stable coordination chemistry of radioactive89Zr4+in an aqueous environment is of paramount importance whendeveloping positron-emitting radiotracers based on proteins (usually antibodies) for use with positron emission tomography.Desferrioxamine B (DFO) remains the chelate of choice for clinical applications of89Zr-labeled proteins, but the coordination ofDFO to Zr4+ions is suboptimal. Many alternative ligands have been reported, but the challenges in measuring very high log valueswith metal ions such as Zr4+that tend to hydrolyze mean that accurate thermodynamic data are scarce. In this work, densityfunctional theory (DFT) calculations were used to predict the reaction energetics for metal ion complexation. Computed values ofpseudoformation constants (log) are correlated with experimental data and showed an excellent linear relationship (R2= 0.97).The model was then used to estimate the absolute and relative formation constants of 23 different Zr4+complexes using a total of 17different ligands, including many of the alternative bifunctional chelates that have been reported recently for use in89Zr4+radiochemistry. In addition, detailed computational studies were performed on the geometric isomerism and hydration state of Zr-desferrioxamine. Collectively, the results offer new insights into Zr4+coordination chemistry that will help guide the synthesis offuture ligands. The computational model developed here is straightforward and reproducible and can be readily applied in the designof other metal coordination compounds.

DOI: https://doi.org/10.1021/acs.inorgchem.9b03515

Predicting the thermodynamic stability of zirconium radiotracers

Jason P. Holland*

University of Zurich, Department of Chemistry, Winterthurerstrasse 190, CH-8057, Zurich, Switzerland

*** Correspondence:**

Prof. Dr Jason P. Holland

Tel: +41.44.63.53.990

E-mail: jason.holland@chem.uzh.ch

Website: www.hollandlab.org

Running Title: *Predicting zirconium radiotracer stabilities*

Abstract

The thermodynamic stability of a metal-ligand complex, as measured by the formation constant (log β) is one of the most important parameters that determines metal ion selectivity and potential applications in, for example, radiopharmaceutical science. The stable coordination chemistry of radioactive $^{89}Zr^{4+}$ in aqueous conditions is of paramount importance when developing positron-emitting radiotracers based on proteins (usually antibodies) for use with positron emission tomography. Desferrioxamine B (DFO) remains the chelate of choice for clinical applications of ^{89}Zr-labelled proteins but the coordination of DFO to Zr^{4+} ions is suboptimal. Many alternative ligands have been reported but challenges in measuring very high log β value with metal ions like Zr^{4+} that tend to hydrolyse mean that accurate thermodynamic data are scarce. In this work, density functional theory (DFT) calculations were used to predict the reaction energetics for metal ion complexation. Computed values of pseudo formation constants (log β′) are correlated with experimental data and showed an excellent linear relationship (R^2-value = 0.97). The model was then used to estimate the absolute and relative formation constants of 23 different Zr^{4+} complexes using a total of 17 different ligands, including many of the alternative bifunctional chelates that have been reported recently for use in $^{89}Zr^{4+}$ radiochemistry. In addition, detailed computational studies were performed on the geometric isomerism and hydration state of Zr-desferrioxamine. Collectively, the results offer new insights into Zr^{4+} coordination chemistry that will help guide the synthesis of future ligands. The computation model developed here is straightforward, reproducible, and can be readily applied in the design of other metal coordination compounds.

Keywords: Density functional theory (DFT), formation constants (log β), thermodynamic stability, metal complexes, zirconium, desferrioxamine B (DFO), radiopharmaceuticals

Introduction

The '*stability'* of metal ion coordination complexes is a critical issue that governs their potential application as drugs, diagnostic imaging agents or molecularly targeted radiotherapeutics. When a metal ion complex is challenged by the harsh environment of the body, the concept of 'stability' becomes non-trivial. An established dogma in radiopharmaceutical science is that kinetic stability of the coordination complex with respect to loss of the metal ion from the ligand is a primary factor that influences the pharmacokinetics of the compound *in vivo*. However, kinetic stability is only one facet of metal complex stability. Other factors that influence the stability and selectivity toward specific metal ion chelation *in vivo* include protonation (pK_a) constants, coordination numbers, counter ion binding, redox stability in the presence of high concentrations of oxidizing or reducing agents such as glutathione or ascorbic acid etc. Metabolic stability also plays an important role. For instance, transchelation of the metal ion to other metal-binding proteins with either higher binding affinity or elevated concentrations can reduce the stability of the complex *in vivo*. Specific enzyme-mediated catabolic reactions (either metal-centred or ligand-centred processes) can also alter the chemical structure of the complex leading to a decrease in both thermodynamic and kinetic stability.

Zirconium-89 ($t_{1/2}$ = 78.41 h) is a positron-emitting radionuclide that has risen to prominence for radiolabelling larger, long-circulating proteins (mainly antibodies) for use in immune-positron emission tomography imaging (immuno-PET).[1] At present, bifunctional derivatives of the nature product siderophore desferrioxamine B (DFO) are the chelates of choice for functionalising proteins and radiolabelling with $^{89}Zr^{4+}$ ions. DFO is an outstanding chelate for $^{89}Zr^{4+}$ and clinical experience with ^{89}ZrDFO-radiolabelled antibodies have proven that the complex is suitable for use in human trials. Nevertheless, computational work provided the first indication

that the Zr-desferrioxamine complex may be suboptimal due to the fact that DFO provides only 6 donor atoms and the Zr^{4+} ion can accept up to 8 donor atoms in the first coordination sphere.[2] Since then, many groups have explored the aqueous phase coordination chemistry of Zr^{4+} with the aim of developing new chelates for improving the stability of $^{89}Zr^{4+}$ ion coordination *in vivo*. Further computation studies probed the thermodynamics and mechanism of the pH-dependent exchange of oxalate anions for hydroxamate ligands, and the results helped to establish a set of design criteria for new chelates with improved thermodynamic and kinetic stability of Zr^{4+} complexation.[3] Several promising new ligands have emerged and the topic has been reviewed.[4–7]

In spite of the various definitions of 'stability', thermodynamic stability remains the ultimate arbiter when comparing the relative stability and metal ion selectivity of different chelates. The justification for this statement is that in a challenge experiment where two chelates compete for a metal ion, given a sufficiently long time, the complex with the lowest free energy of formation in the conditions of the experiment ($\Delta_f G$ / kJ mol^{-1}, or equivalently the largest formation constant, log β [dimensionless]) will predominate. It is perhaps surprising that measurements of the thermodynamic formation constants (log β) for Zr-ligand complexation reactions are rarely performed.[8–10] In part this absence of thermodynamic data is explained by the challenges of measuring formation constants for Zr^{4+} ions. The high charge-to-size ratio of the Zr^{4+} ion means that it forms complexes with extremely high thermodynamic stability that cannot be easily (or directly) determined using standard potentiometric titrations. Ligand competition methods are required and this poses the problem of selecting an appropriate competing ligand for which the formation constant is known accurately and whose metal complex is kinetically labile to facilitate transchelation on a reasonable experimental time scale. Furthermore, Zr^{4+}(aq) ions are highly acidic and readily hydrolyse leading to insoluble Zr-oxide species that precipitate from

solution. Finally, the d^0 electron configuration of the Zr^{4+} ion means that many of the complexes are essentially colourless with no useful spectroscopic handle to follow the complexation process by either electronic absorption or fluorescence emission methods (exceptions using HOPO ligands are noted[11,12]). Isothermal calorimetry (ITC) methods can be used to determine formation constants but the technique is non-trivial, especially when using highly acidic cations that are prone to precipitation. For redox active metal complexes, cyclic voltammetry can also be used. Variations in the experimental conditions (temperature, acid/base composition, ionic strength, electrolyte, analyte concentrations etc) also mean that it is not always possible to compare the values of complex formation constants determined from different procedures.

Computational chemistry offers an alternative approach for estimating the relative (and potentially absolute) thermodynamic stability of different metal ion complexes.[13,14] Predicting absolute values of formation constants is notoriously difficult.[14] To illustrate the problem, a difference of one log unit in the formation constant ($\Delta(\log_{10} \beta) = 1$) is equivalent to only 5.7 kJ mol^{-1} in the standard formation free energy ($\Delta_f G$; at T = 298.15 K). Coupled with the aforementioned variations in experimental measurements, this means that calculated estimates of formation constants (and indeed other equilibrium processes like the determination of absolute protonation constants – p*K*a values[15,16]) lies at the limit of chemical accuracy of current computational methods. In addition, predicting formation constants requires accurate calculations of hydration enthalpies for the various water clusters, metal aquo ions, free ligands and metal ion coordination complexes. All ligands that are currently used to complex Zr^{4+} ions involve acidic donor groups (carboxylic acids, hydroxamic acids, hydroxypyridinoic acids, etc) which imposes a problem of calculating the structure of the 'free' ligand. Finally, most metal ion complexes like Zr-desferrioxamine often exhibit a high degree of structural isomerism. Collectively, these

challenges mean that successful computational models for estimating absolute and relative formation constants must be benchmarked to experimental data. This work develops a new computational approach to predict the absolute and relative thermodynamic stability (calculated log β values) of Zr^{4+} complexes *via* correlation to experimentally validated systems. Geometric isomerism for the 6-, 7- and 8-coordinate model complexes of $[ZrDFO(H_2O)_n]$, (where n = 0, 1 or 2) is studied. Finally, computational modelling was used to estimate the absolute and relative thermodynamic stability of 23 Zr^{4+} complexes including many of the promising alternative chelates that have been reported in recent years.

Computational Methods

All calculations were conducted by using density functional theory (DFT) as implemented in the Gaussian16 Revision A.03 suite of *ab initio* quantum chemistry programs. Normal self-consistent field (SCF) and geometry convergence criteria were employed throughout. Structures were optimised without using symmetry constraints. All structures were optimised in solution phase using the integral equation formalism polarisable continuum model (IEFPCM) initially developed by Tomasi and co-workers.[17] Solvated phase calculations were implemented by using the SCRF keyword with default parameters, and selecting water as the solvent (dielectric constant, $\varepsilon = 78.39$, and solvent sphere radius, $R_{solv} = 1.385$ Å).[18] The solute-solvent boundary was defined by using a solvent excluding surface (SES).[19] Harmonic frequency analysis based on analytical second derivative was used to characterise all optimised structures as local minima on the potential energy surface. Calculations were performed using the B3LYP[20–22] exchange-correlation (XC) functionals and the all-electron double-ζ DGDZVP[23,24] basis set. The choice of solvation model reflects the typical conditions of radiosynthesis and subsequent application of metal-based

radiopharmaceuticals *in vivo*. Optimised structures and molecular orbitals were analysed by using Chemcraft (version 1.8, build 536b, www.chemcraftprog.com).

Results and Discussion

The model reaction

The standard reaction defining the thermodynamic formation constant in water is given in Equation 1 where the formation constant β is given by Equation 2 (note strict thermodynamic definitions should use species activity and not concentrations).

$$[\mathrm{M(H_2O)}_x]^{a+} + \mathrm{H}_b\mathrm{L} \rightleftharpoons [\mathrm{ML}]^{(a-b)+} + b\mathrm{H}^+ + x(\mathrm{H_2O}) \qquad \text{(Equation 1)}$$

$$\beta = \frac{[[\mathrm{ML}]^{(a-b)+}]}{[\mathrm{M}^{a+}][\mathrm{H}_b\mathrm{L}]} \qquad \text{(Equation 2)}$$

Hence, if one can calculate the free energy of each species present, then computational methods can be used to estimate the formation constant. In practice, there are many problems that need to be addressed before DFT method can be used to compute a log β value for a given complexation reaction. All species in Equation 1 are solvated so the nature of the solvation model (explicit or implicit) must be defined. As the ligand binds the metal ion, water molecules are released which means that one must compute an appropriate water cluster model. While DFT may perform better than expected, this remains non-trivial.[25–27] The structure and energetics of the metal-aquo ion complex must be calculated and accuracy has been shown to be dependent on the complex ion geometry as well as the number of explicit of solvation shells included in the calculated structures.[28–31] The geometry of the free ligand must be estimated. In many cases, and especially for acyclic ligand systems, an extremely large number of possible conformers exist as an ensemble in solution under ambient conditions. If the effects of varying protonation states of the free ligand are also to be included, this means that identifying an accurate and appropriate minimum energy

structure on potential energy surface is an extreme challenge. The ML complexes themselves often exist as multiple geometric and conformational isomers with varying aquo ligands, solvation states and differences in non-coordinating counter ions. Finally, if Equation 1 is to be applied in full, one must consider how to account for the energy of the solvated proton. Taken together, these challenges mean that a comprehensive computational approach for the determination of absolute formation constants is beyond the reach of current theory. To develop a practical computational approach that is applicable to large metal ion complexes like Zr-desferrioxamine, and may be used to facilitate the design of new ligand systems, simplifications are needed and correlation with experimental data is essential.

The computational approach developed herein uses the model reaction given by Equation 3.

$$[\mathrm{M(H_2O)}_n]^{a+} + \mathrm{L}^{b-} \rightleftharpoons [\mathrm{ML}]^{(a-b)+} + n(\mathrm{H_2O}) \qquad \text{(Equation 3)}$$

The system uses two simplifications to facilitate reproducible estimates of reaction free energies ($\Delta_r G$ / kJ mol^{-1}) for the complexation step and hence estimation of calculated pseudo-formation constants (log β′ values). First, the ligand is defined in the deprotonated state whereby all the protons associated with all acidic donor groups that coordinate to the metal ion have been removed. This simplifies and standardises the approach taken for the calculation of the geometry and energetics of the free ligand L^{b-}. Importantly, it also offers a way of defining the initial geometry of the free ligand (taken from the optimised structure of the complex with the metal ion removed) in a way that can be reproduced across ligands and complexes that may have very different structures. Second, by using a deprotonated ligand as the energy reference species it removes the complications associated with calculating the structure and energetics of the solvated protons.

The concept is to first use this simplified and reproducible computational model to estimate the reaction free energy ($\Delta_r G$ / kJ mol^{-1}, and hence a calculated pseudo formation constants log β′), and then correlate the results to experimental values to obtain a calibration plot that can then be used to estimate both absolute and relative formation constants for complexation reactions using new ligands. The following sections describe calculations on each of the four components required to satisfy Equation 3.

Water clusters

The geometric and electronic structure of water is one of the most difficult problems to compute water clusters remains an active field of research.[25–27] High level calculations can be used to obtain improved results[27,32] but estimating formation constants means that the computational method must be appropriate and affordable for the calculation of large metal ion complexes. Hence, DFT methods were employed here[26] although care should be taken when selecting the combination of exchange-correlation functionals and basis set.[33] Previous work established that the combination of the B3LYP exchange-correlation functionals with the DGDZVP basis gave acceptable results when calculating the structure, electronic properties and reactivity of Zr^{4+} complexes.[3]

The structures of water clusters $n(H_2O)$, where n = 1 to 16, were optimised for use as energy reference points. Input structures were adapted from the comprehensive structure survey reported by Maheshwary *et al*.[25] For each cluster, the relative calculated electronic energy (Δε(SCF)), zero point energy (ZPE), free energy, enthalpy and entropy per water molecule are given in Table S1 and plotted in Figure 1. The important feature was to define a range of water cluster sizes for which the difference in computed energy per water molecule was as small as possible. For example, if complexation leads to the formation of a water cluster with ca. 2 or 6 water molecules, then the

contribution from the water cluster to the computed free energy could vary by as much as 8.19 kJ mol^{-1} per water molecule – this is equivalent to a difference of 1.4 in the value of the computed pseudo log β′ or subsequently the estimated log β values. As can be seen from the values of the ΔG / kJ mol^{-1} per water molecule in Table S1, clusters of sizes 8, 9 and 10 water molecules have similar energies and can be used as energy reference points without introducing large variations in the calculated reaction free energies, enthalpies or entropies.

Figure 1. Plot of the relative calculated energy per water molecule *versus* water cluster size ($n(H_2O)$, where n = 1 to 16). Note, *H*, *S*, and *G* refer to the enthalpy, entropy and Gibb's free energy, respectively.

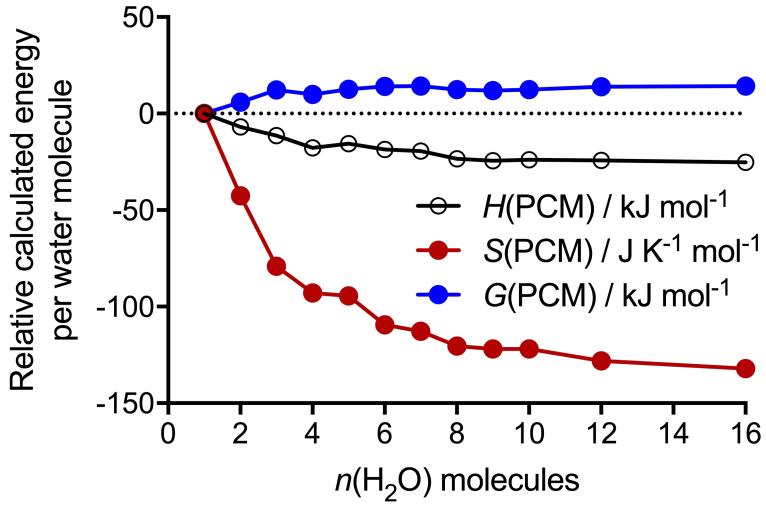

Metal-aquo complexes

The structures of several metal-aquo cations including Zn^{2+},[28] Cu^{2+},[34,35] Mg^{2+},[29,31] and Al^{3+} ions, [30,31] and the effects of incorporating sequential first, second and third hydration shells has been studied in detail. For an octahedral metal ion complex with 6 water molecules in the first coordination sphere and 12 water molecules in the second shell, Bock *et al*. reported that a structure

with S_6 symmetry was energetically more stable than structures with tetrahedral (T_h or T) symmetry.[29,30] However, Beret *et al.* noted that if a partial third hydration shell comprising of an additional 24 water molecules is added to $[M(H_2O)_{18}]^{a+}$ complexes where M = Mg^{2+} or Al^{3+} ions (and a = 2+ or 3+), the resulting $[M(H_2O)_{42}]^{a+}$ species (42 water molecules in total) converged with the lowest energy structures displaying T_h symmetry for the embedded $[M(H_2O)_{18}]^{a+}$ unit.[31] It is important to note that addition of a third hydration shell leads to an exponential increase in the number of potential conformers. Also, 24 additional water molecules are insufficient to provide a complete hydrogen bonding network in the third shell. Therefore, whilst significant improvements may be obtained in the description of the structures and energies of metal-aquo species by computing cations with an explicit second solvation shell, addition of a third hydration layer is expected to deliver only marginal benefits for comparatively a large increase in computational expense. Hence, in this work all metal-aquo complexes were computed with explicit first and second hydration shells (Figure 2). Note that with the exception of Zr^{4+} ions, the structures of all other metal-aquo complexes were calculated as the $[M(H_2O)_{18}]^{a+}$ species. For Zr^{4+} ions, the tendency to expand the first coordination sphere was evident in the optimised structure of $[Zr(H_2O)_{18}]^{4+}$ (a = 4+) which displayed a pronounced displacement of the Zr^{4+} ion toward one face of the S_6 water cluster. Therefore, to 'cap' this vacant coordination site, additional water molecules were introduced. Formation of a 7-coordinate Zr^{4+} species, $[Zr(H_2O)_{19}]^{4+}$ with 7 first coordination sphere water molecules bound to the central metal ion was found to be stable (Figure 2B). In contrast, no stable minimum was identified for Zr^{4+} ions when starting structures contained 8 water molecules in the first shell.

Figure 2. Structures of the metal-aquo ion complexes $[M(H_2O)_n]^{a+}$ (where n = 18 or 19) with twelve H_2O molecules in the second solvation shell and either (A) 6-water molecules, or (B) 7-water molecules in the first coordination sphere. Note the structure in (A) has S_6 symmetry but no symmetry constraints were imposed in the calculations (all molecules were calculated with C_1 symmetry).

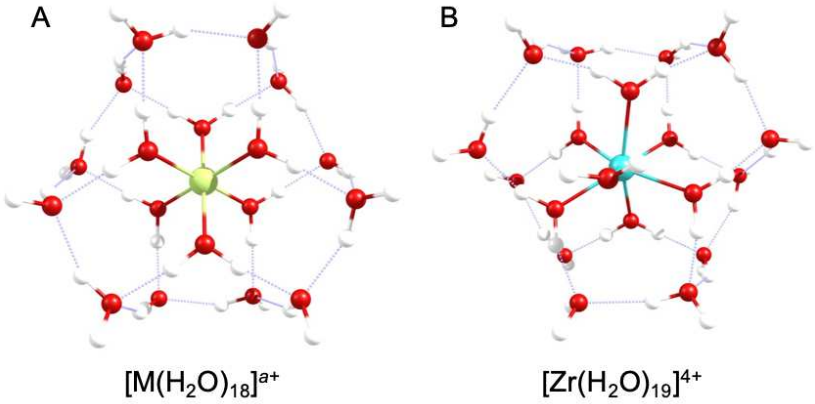

Isomerism and hydration of the Zr-desferrioxamine complex

Previous computational work indicated that the Zr-desferrioxamine complex can potentially coordinate two additional ligands forming an 8-coordinate species.[2] It was noted that one of the water molecules appeared to be tightly bound in a pseudo-axial coordination site whereas the second water molecule had an elongated *r*(Zr–O) bond length and was likely to be highly labile under ambient conditions in aqueous solution. These former calculations started from a geometry derived from the experimental single-crystal X-ray structure of FeDFO[36] and did not take into account potential geometric isomerism about the metal-DFO coordination.[37] Therefore, before proceeding to calculate the formation constants of different metal complexes, structural isomerism was investigated for the $[ZrDFO(H_2O)_n]^+$ model complexes where n = 0, 1 or 2 (Figure 3). Note that for all calculations a model DFO complex was used whereby the terminal $–(CH_2)_5NH_3^+$ chain

of native DFO that is used to conjugate to proteins *via* chemistry at the primary amine was replaced with a methyl group. Optimised structures for the geometric isomers $[ZrDFO(H_2O)_n]^+$ model complexes with either 6-coordinate (n = 0), 7-coordinate (n = 1), or 8-coordinate (n = 2) structures are presented in Figures 4, 5 and 6, respectively. Similarly, plots of the relative calculated differences in free energy (blue lines), enthalpy (black lines) and entropy (red lines) for the different geometric isomers of the 6-, 7- and 8-coordinate $[ZrDFO(H_2O)_n]^+$ model complexes are presented in Figures 7, 8 and 9, respectively. Note, all energies are plotted relative to the *N-cis-cis* isomer. Complete data are presented in supporting information Tables S3, S4 and S5.

Figure 3. Structures of the 8 possible geometric isomers when DFO coordinates to Zr^{4+} ion (or other metal ions) to form an octahedral complex. Note, all isomers are optically active and only structures for the Λ-enantiomers are presented. Hence, in total, there are 16 possible stereoisomers of the $[Zr(DFO)]^{+}$ complex. The nomenclature used to describe each isomer is consistent with that reported by Borgias *et al*.[37]

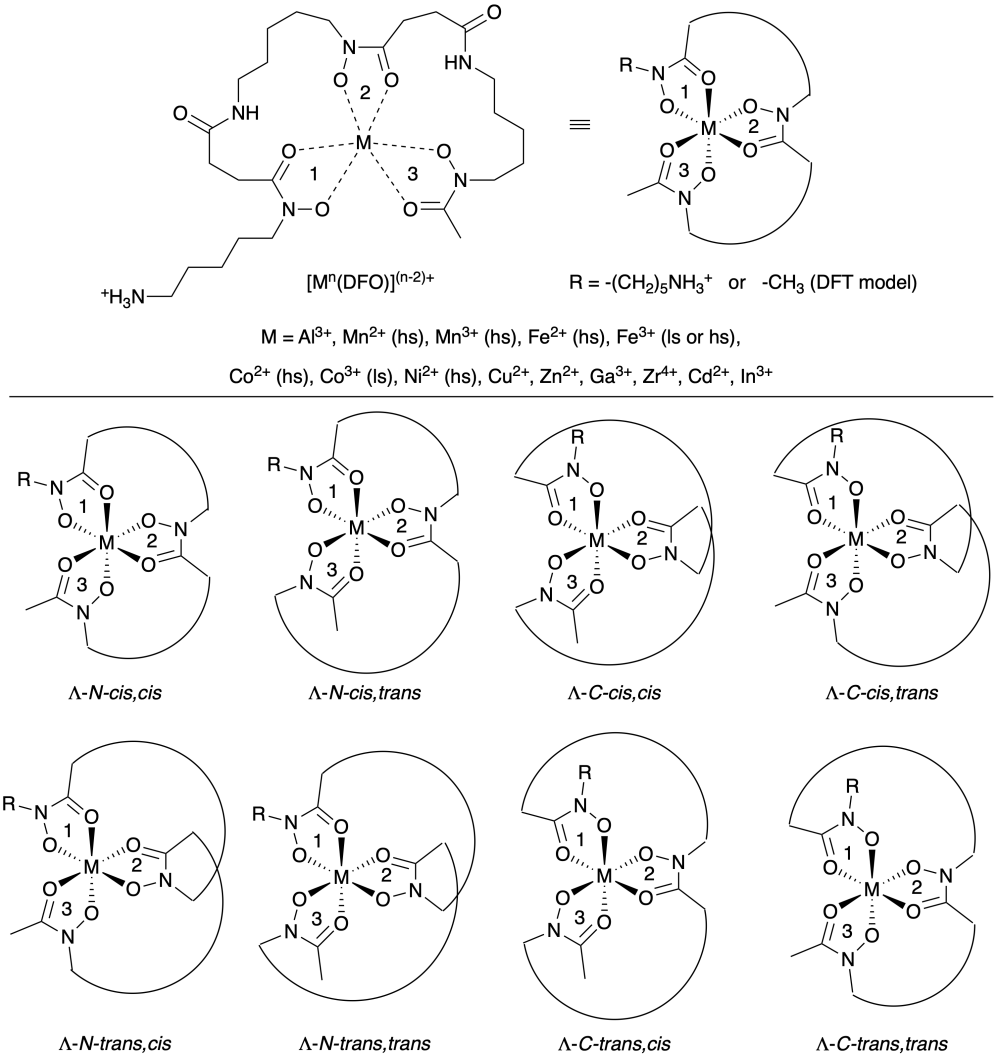

Figure 4. Pictures of the optimized geometric isomers of the 6-coordinate $[Zr(DFO)]^+$ complex.

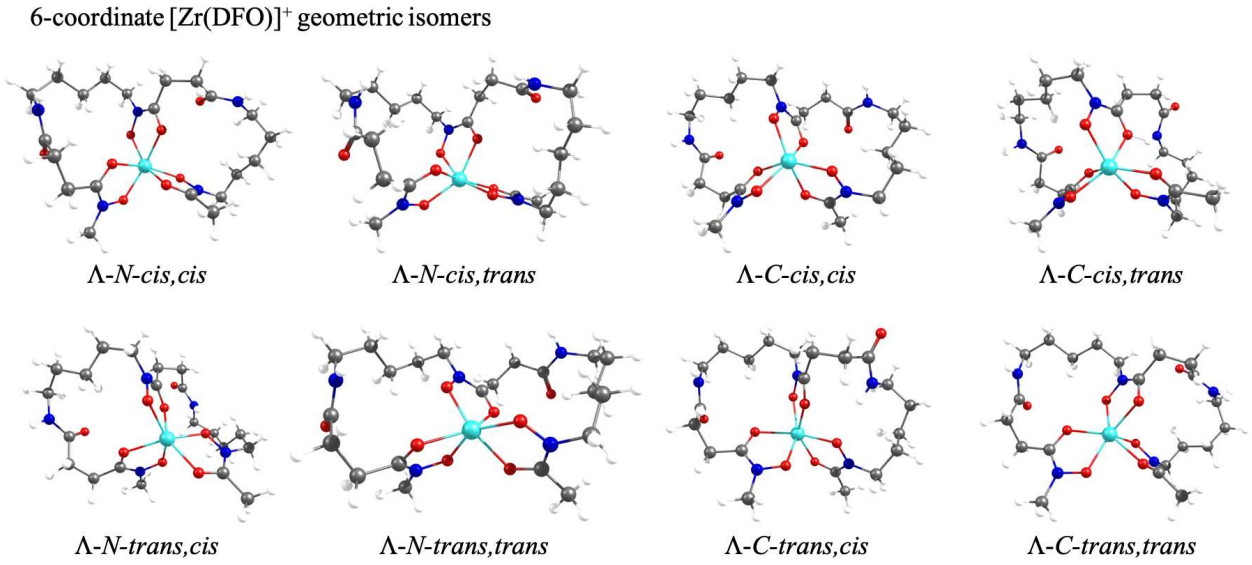

Figure 5. Pictures of the optimized geometric isomers of the 7-coordinate $[Zr(DFO)(H_2O)]^+$ complex.

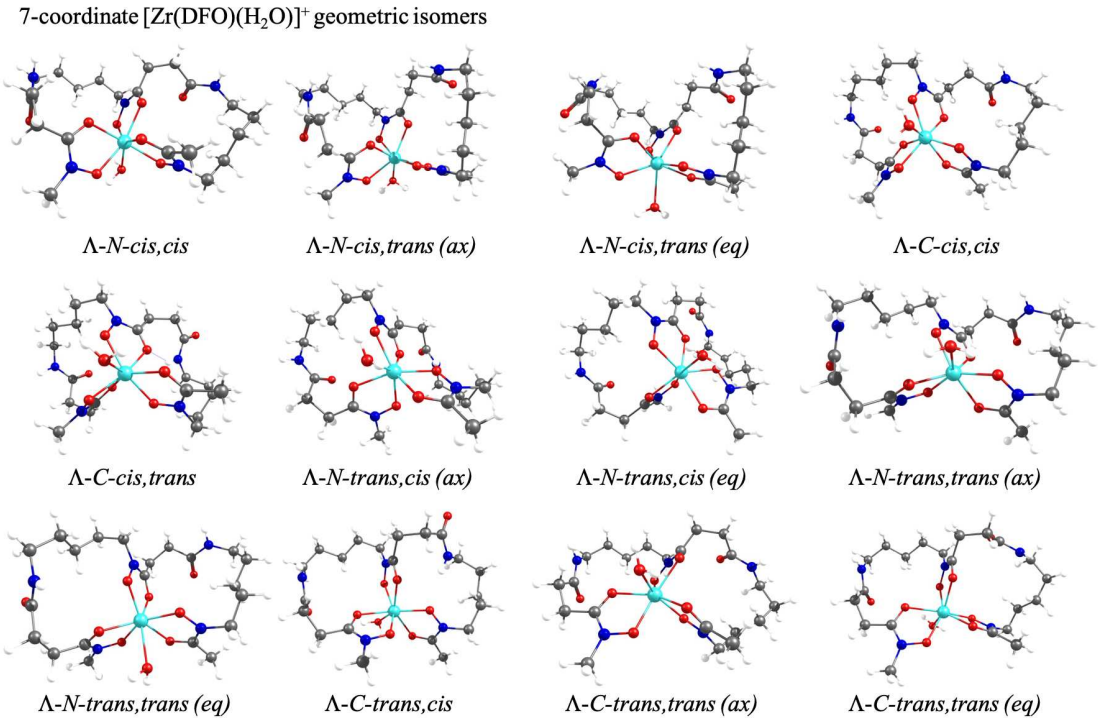

Figure 6. Pictures of the optimized geometric isomers of the 8-coordinate $[Zr(DFO)(H_2O)_2]^+$ complex.

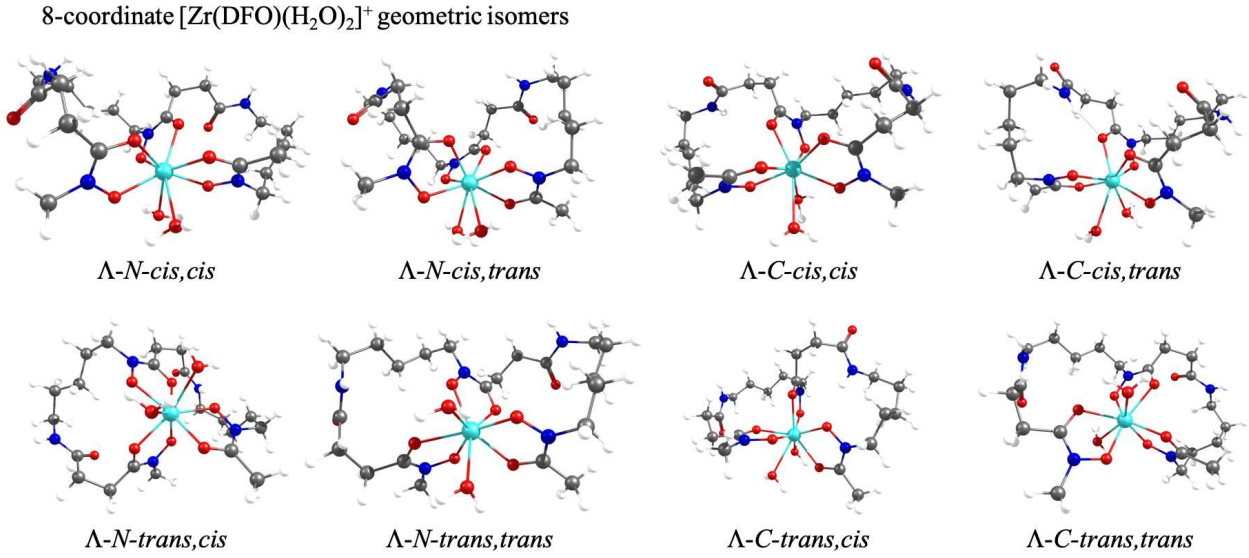

Figure 7. Plot of the relative calculated energies of the different geometric isomers of the 6-coordinate $[Zr(DFO)]^+$ complex. Energies are given in Table S3 and optimized structures are shown in Figure 4.

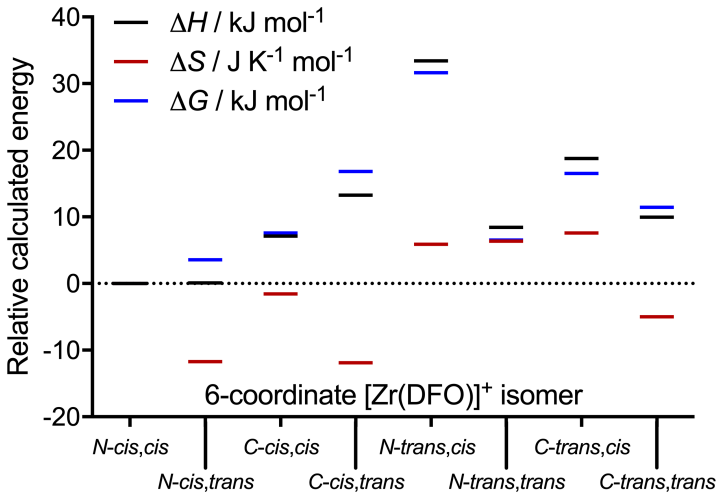

Figure 8. Plot of the relative calculated energies of the different geometric isomers of the 7-coordinate $[Zr(DFO)(H_2O)]^+$ complex. Energies are given in Table S4 and optimised structures are shown in Figure 5. Unless otherwise stated, the coordinated water molecule is located in a pseudo-axial site.

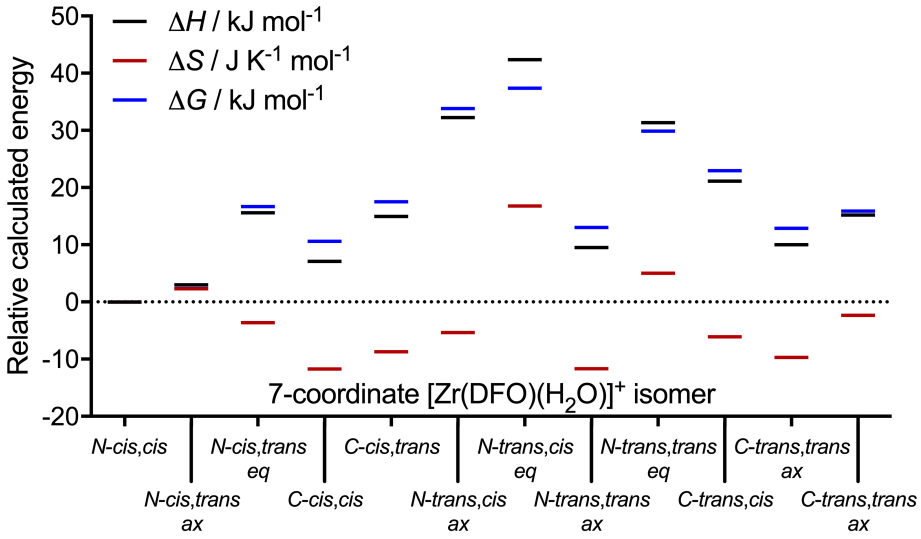

Figure 9. Plot of the relative calculated energies of the different geometric isomers of the 8-coordinate $[Zr(DFO)(H_2O)_2]^+$ complex. Energies are given in Table S5 and optimized structures are shown in Figure 6.

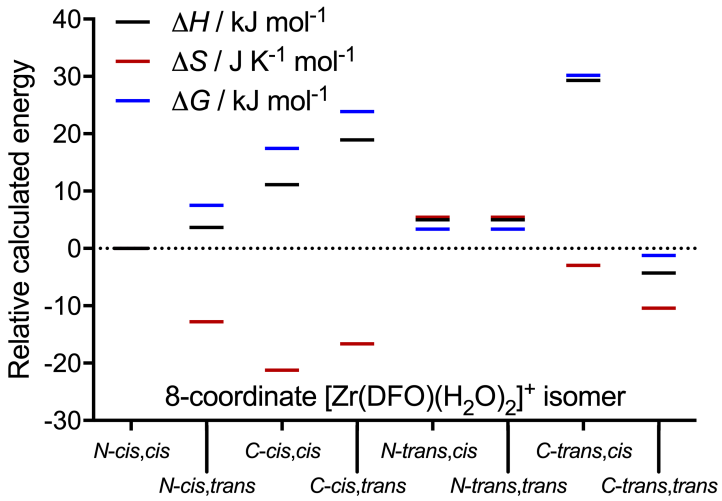

For 6-coordinate $[ZrDFO]^+$ the *N-cis-cis* isomer is calculated to be the most stable structure. However, it is worth noting that with the exception of the *N-trans-cis* isomer, all other structures lie within 20 kJ mol^{-1} of the minimum energy structure. As such, the DFT calculations suggest that Zr^{4+} ion complexation by DFO is likely to produce a range of different structures in solution phase.

Addition of one water molecule led to 7-coordinate $[ZrDFO(H_2O)]^+$ species in which for most isomers, the coordinated water molecule could occupy either a pseudo-axial (ax) or pseudo-equatorial (eq) binding site (Figures 5 and 8). Again, the *N-cis-cis* isomer with a pseudo-axial water molecule was calculated to be the most stable geometry. In contrast to the 6-coordinate isomers, larger variations in energy are seen with the least stable 7-coordinate species being the *N-trans-cis* isomer with a pseudo-equatorial coordinated water molecule. Nevertheless, the energetic plot in Figure 8 shows that at least 8 geometric isomers lie within 20 kJ mol^{-1} free energy and it is likely that multiple isomers co-exist in aqueous solution under ambient conditions.

For the 8-coordinate $[ZrDFO(H_2O)_2]^+$ species, with the exception of the *C-trans-trans* isomer in which the two water molecule were bound in a trans configuration, the lowest energy minimum for all other structures converged with the two coordinated water molecules occupying a *cis* geometry (Figures 6 and 9). In most cases, attempts to coordinate the two water molecules with *trans* orientation (occupying both pseudo-axial sites) led to the dissociation of one water molecule due to electronic and steric repulsion. In general, the pseudo-trigonal face of the complex in which two or more N-O donor groups are located is more open than the face occupied by more carbonyl (C=O) donors.

The wide range of energetically similar geometric isomers with coordination numbers ranging from 6- to 8-donor atoms in the first coordination sphere is, in part, a plausible explanation

as to why all attempts to crystallise the Zr-desferrioxamine complex have (so far) failed. These data also highlight the importance of understanding structural isomerism in metal-ligand complexes – particularly if computational tools are used to 'design' new ligand systems. Note, the energetics of the most stable isomers were used in the calculations of all formation constants for DFO derivatives. Use of higher energy complexes would tend to underestimate the formation constant.

Calibration with experimental data

To produce a working computational, the reaction energetics for the formation of 14 different metal-DFO complexes, as well as that for the ZrTHPN complex[10,38] were calculated in accordance with Equation 3 and compared with experimental data. Data are presented in Table 1 and are plotted in Figure 10. These absolute calculated values of the pseudo formation constant log β′ are likely to be overestimated *versus* experimental data. However, an excellent linear correlation was observed with a correlation coefficient (R^2-value) of 0.97, a slope of 1.985±0.095 and a *y*-intercept of 45.48±2.47 (Figure 10A). A plot of the residuals from the linear regression analysis revealed no systematic errors (Figure 10B). The data were used to generate Equation 4, which for this computational methodology, allows the estimation of formation constants with a standard deviation of 2.21 log β units (equivalent to a standard deviation of only 12.6 kJ mol^{-1} in the calculated reaction free energies, $\Delta_r G$).

$$\log \beta_{\text{estimated}} = \frac{(\log \beta' - 45.48 \pm 2.47)}{1.985 \pm 0.095} \qquad \text{(Equation 4)}$$

A plot of the computationally estimated formation constants versus experimentally determined formation constants (log β) is shown in Figure 10C. The tight correlation between the DFT calculations and the experimental data, and the wide range of formation constants covered by the

model, which encompasses experimental values ranging from log β = 7.68 for the high-spin $[Mn(DFO)]^{-}$ complex to 50.3 for Zr(THPN), strongly suggest that this approach gives reliable estimates for both the absolute and relative formation constants.

Figure 10. (A) Plot of the calculated pseudo formation constant log β′ *versus* the experimentally measured values for different metal DFO complexes and Zr(THPN). Corresponding data are given in Table 1, and results from the linear regression analysis are shown inset with the prediction bands set at 95% confidence. (B) Plot of the residuals from the linear regression analysis. (C) Plot of the estimated formation constants (log β) *versus* the experimental values.

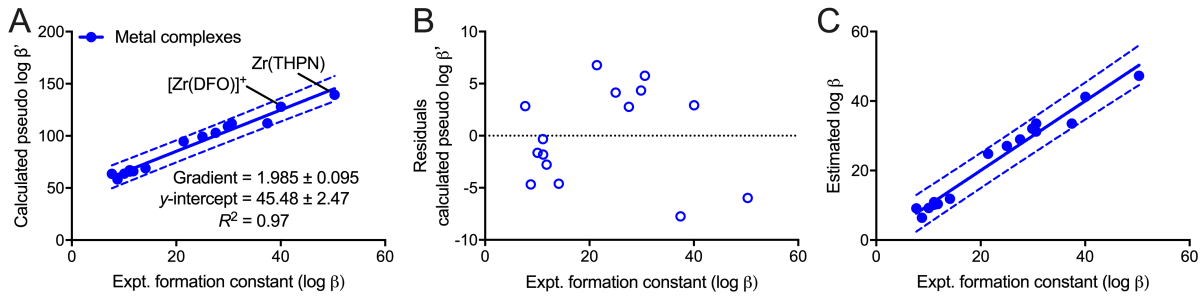

Table 1. Calculated reaction energetics for the formation of several metal-DFO complexes in accordance with Equation 3. Computed values of the calculated pseudo log β′ values are correlated linearly with experimental data and the linear model was used to produce the estimated values of log β in accordance with Equation 4.

B3LYP/DGDZVP/PCM	Calculated thermodynamics of complex formation (T = 298.15 K)								
Complex (model DFO)	Δε(SCF) / kJ mol^{-1}	ΔZPE / kJ mol^{-1}	ΔG / kJ mol^{-1}	ΔH / kJ mol^{-1}	ΔS / J K^{-1} mol^{-1}	Calculated pseudo log β′	Estimated log β	Experimental log β[b]	Deviation (Estimated – Expt.)
Al(DFO)	-520.38	4.51	-566.55	-518.71	160.44	99.24	27.08	25.0	2.08
[Mn(DFO)]$^-$ hs	-322.16	6.36	-362.93	-326.54	122.06	63.57	9.11	7.68	1.43
Mn(DFO) hs	-573.23	3.94	-623.01	-570.40	176.48	109.13	32.07	29.88	2.19
[Fe(DFO)]$^-$ hs	-340.81	-4.22	-383.40	-343.45	134.01	67.16	10.92	11.09	-0.17
Fe(DFO) hs	-592.29	0.75	-639.24	-589.27	167.60	111.98	33.50	30.6	2.90
Fe(DFO) ls[a]	-566.09	4.58	-613.71	-561.98	173.50	107.50	31.24	30.6	0.64
[Co(DFO)]$^-$ hs	-322.77	3.83	-364.23	-326.55	126.37	63.80	9.23	10.06	-0.83
Co(DFO) ls	-583.81	3.02	-639.82	-576.76	211.48	112.08	33.55	37.45	-3.90
[Ni(DFO)]$^-$ hs	-332.60	1.94	-377.30	-335.31	140.84	66.09	10.38	11.78	-1.40
[Cu(DFO)]$^-$	-353.23	5.31	-393.99	-357.61	122.04	69.02	11.86	14.1	-2.24
[Zn(DFO)]$^-$	-330.28	3.85	-375.11	-333.75	138.74	65.71	10.19	11.1	-0.91
Ga(DFO)	-543.20	1.58	-587.73	-541.05	156.58	102.95	28.95	27.56	1.39
[Zr(DFO)]$^+$	-679.3	9.40	-726.5	-677.90	162.86	127.26	41.20	40.04	1.16
Zr(THPN)	-752.69	10.35	-795.45	-753.13	141.93	139.34	47.28	50.3	-3.02
[Cd(DFO)]$^-$	-284.70	2.93	-332.26	-287.10	151.46	58.20	6.41	8.76	-2.35
In(DFO)	-488.55	0.63	-540.79	-486.31	182.72	94.73	24.81	21.4	3.41

[a] The low spin [Fe(DFO)]$^+$ complex was not used in the correlation between the computational model and the experimental data. [b] Note values for the experimental formation constants were obtained from several sources including Buchwalder *et al*.,[38] Schwarzenbach *et al*.,[39] Anderegg *et al*.[40] Evers *et al*.,[41] Zu and Hider,[42] Kruft *et al*.[43], Hernlem *et al*.[44], Duckworth *et al*.,[45] and references therein.

Predicting the absolute and relative formation constants of zirconium complexes

In total, optimised structures and reaction energetics for 23 different Zr^{4+} complexes, using 17 different ligands (Figure 11) were calculated.[2,10,38,46–62] Structures of the optimised Zr-complexes are presented in Figure 12 and key thermodynamic data are given in Table 2. The ligands chosen were selected based on their reported experimental potential to form stable complexes with $^{89}Zr^{4+}$ ions and also based on their availability as bifunctional versions that can be coupled to protein. For each complex, the reaction energetics, the calculated pseudo log β′ (from Equation 3) and the estimated log β values (from Equation 4) are presented. Based on the calculated data, the relative thermodynamic stabilities of the complexes are ranked in order from highest to the lowest. For convenience of interpreting the results, data are also plotted in Figure 13 with DFO-based chelates grouped on the right and alternative ligands shown on the left.

When inspecting the data, several interesting features and trends emerge. Firstly, as predicted previously, 8-coordinate complexes display higher formation constants than 6-coordinate species (as can be inferred from enthalpic and entropic arguments). This is highlighted by comparison of the calculated formation constants for the Zr-complex of DFO*.[60] Optimised structures of Zr(DFO*) were calculated with either three (6-coordinate) or four (8-coordinate) of the hydroxamate groups bound to the central metal cation with corresponding estimated log β values of 40.37 and 51.56, respectively. As long as other steric and electronic factors allow for favourable orientation of 8-donor atoms around the Zr^{4+} ion, these 8-coordinate isomers are likely to be formed. However, it is interesting to note that the average binding energy for the first 3 hydroxamate groups of DFO* to Zr^{4+} is ΔG_{ave} = -239.0 kJ mol^{-1} whereas the average free energy per hydroxamate group for the 8-coordinate complex is only -211.0 kJ mol^{-1}. The effects of steric and electronic repulsion in the 8-coordinate complex mean that coordination of the 4th

hydroxamate group stabilises the complex by an additional -126.8 kJ mol^{-1} which is 112.3 kJ mol^{-1} less than the average stabilisation obtained from coordination of the first three hydroxamate groups.

Desferrioxamine B performs very well and in spite of some of the comments that have appeared in recent literature, DFO remains an excellent chelate for coordination of Zr^{4+} ions. The calculated formation constant of log β = 41.20 is in excellent agreement with the recent experimental measurement of 40.04 reported by Toporivska *et al*.[8] The deviation between the calculated value and the experimental measurement is only +1.16 log β units which corresponds to a deviation in the reaction free energy of only 6.6 kJ mol^{-1} – which is at the limits of chemical accuracy using DFT methods.

Codd and co-workers were the first to incorporate ether groups into backbone of the DFO ligand converting the $–(CH_2)_5–$ units into $–(CH_2)_2O(CH_2)_2–$ groups forming the DFO-O_3 ligand.[62] This chemical functionalisation has two important effects. First, the ether groups improve the water solubility of the DFO constructs. Second, inserting ether groups in the alkyl backbone improves ligand flexibility which reduces the steric constrains imposed by the DFO-O_3 ligand when it coordinates to the Zr^{4+} ion. Contrary to popular misconceptions, DFO may be a large linear molecule but calculations show that it only just fits around the Zr^{4+} ion. Extending the ligand backbone length or introducing more flexible groups like ethers are two potential avenues for improving the stability of metal complexes with DFO derivatives. The stabilising effect of introducing the ether groups into the DFO backbone can be seen when comparing the estimated formation constants of 6-coordinate $[Zr(DFO\text{-}O_3)]^+$ (log β = 43.37) *versus* the most stable structure of Zr^{4+} complexes with native DFO – the 7-coordinate $[ZrDFO(H_2O)]^+$ species (log β = 41.51). In terms of the calculated change in reaction free energies, formation of $[Zr(DFO\text{-}O_3)]^+$ is more

favourable than $[ZrDFO(H_2O)]^+$ by -21.1 kJ mol^{-1}. A similar effect is also observed for the comparison of the formation constants between Zr(DFO*) (log β = 51.56) and Zr(oxDFO*) (log β = 54.16) with a difference in reaction free energies of $\Delta(\Delta_r G)$ = -26.5 kJ mol^{-1}.

Calculations indicate that thermodynamically, the most stable Zr^{4+} complex is formed by complexation with the oxDFO* chelate. Notably, Zr(DFO-HOPO) has a calculated formation constant of log β = 53.51 and Zr(CTH36) of log β = 52.84. If the same strategy of introducing ether groups into the DFO-HOPO backbone were to be employed (producing an analogue oxDFO-HOPO ligand), the DFT calculations predict that this hypothetical "Zr(oxDFO-HOPO)" complex would likely be the most stable species based on current ligand designs.

Rudd *et al.* reported the synthesis of DFO-squaramide (DFOsqOEt) and suggested that the Zr^{4+} complex with this ligand is 8-coordinate.[49] The DFT optimised structures of $[Zr(DFOsqOEt)]^+$ all converged with a 7-coordinate geometry whereby only one of the oxygen atoms of the 'squarane' unit was bound to the Zr^{4+} ion (Figure 12). No stable minimum was identified in which the central metal ion was 8-coordinate.

The calculations reported here shed new light on the structural isomerism of the Zr-desferrioxamine complex. Recently, Racow *et al.* reported that a 7-coordinate $[ZrDFO(H_2O)]$, bearing one coordinated water molecule could be observed by mass spectrometry.[57] This is consistent with the calculations in which mapping the full reaction energetics for Zr^{4+} ion complexation revealed that the most stable species is actually a 7-coordinate $[ZrDFO(H_2O)]^+$ complex in which the DFO ligand has an *N-cis-cis* geometry about the central metal cation and the water molecule occupies a pseudo axial site (Figures 5 and 8, and Table S4). The experimental and computational data are now in agreement.

Of the alternative chelates, the Zr^{4+} complexes with CTH36 and THPN ligands appear to be the most promising candidates based on the calculated thermodynamics of complex formation. The Zr(CTH36) structure (Figure 12) exhibits a highly symmetric geometry with near ideal D_{2d} symmetry when considering the atoms in the first coordination shell. The Zr^{4+} ion in Zr(CTH36) has the closest geometry to the lowest energy structure of $Zr(MeAHA)_4$ for which crystallographic data were reported by Guerard *et al*.[63,64]. Computational work showed minor differences in the energies of the different geometric isomers $Zr(MeAHA)_4$ which lacks steric constrains in the first coordination sphere and in the ligand.[3] The Zr(CTH36) complex is macrocyclic which means that complexation of Zr^{4+} ion incurs a reduced entropic penalty compared with many acyclic chelates. This is supported by the fact that the change in reaction free entropy, $\Delta_r S$, for Zr(CTH36) formation has the highest value for all complexes studied (264.8 J K^{-1} mol^{-1}, Table 2). Notably, the CTH36 ligand has 8 atom chains between each of carbonyl (C=O) and N-O donor groups. This increased flexibility reduces steric strain in the complex and allows the donor atoms to adopt a preferred geometry. As with the DFO-HOPO ligand, it is likely that introducing ether groups into the CTH36 ligand backbone will enhance ligand flexibility leading to improvements in thermodynamic stability of the Zr complex, and potentially higher water solubility. Subtle effects of ether and thioether groups on the solubility and lipophilicity characteristics of cyclic siderophores were recently reported by Brown *et al*.[65]

It is worth noting that almost all of the new chelates that have been reported to coordinate Zr^{4+} showed improved 'stability' when compared with DFO in ligand challenge experiments. Such chelate challenge experiments are not standardised and reflect only the conditional stability (or formation constants) where the results are dependent on the experimental design. Indeed, it may be that for practical applications, some of these new chelates offer potential advantages over DFO

but the caveat is that one must always take into consideration the experimental conditions employed during the assay. For instance, experiments have shown that DTPA and EDTA can readily transchelate Zr^{4+} from the Zr-desferrioxamine complex but that the process and the reaction kinetics are highly dependent on ligand concentrations and pH. Under slightly acidic conditions, the hydroxamate groups of DFO (and similar DFO-derivatives) are more readily protonated than the carboxylate groups of DTPA and EDTA. Protonation (at ca. pH5-6) reduces the binding affinity of DFO to Zr^{4+} ions while at the same pH carboxylate groups remain essentially fully ionised and available for coordination. Yet, under conditions relevant for applications *in vivo* (pH7.4) the Zr-desferrioxamine complex is favoured and remains stable to DTPA and EDTA challenges. The lesson is that when performing chelate challenge assays, care must be taken to ensure that the pH, temperature, ionic strength, ligand and metal ion concentrations, etc are tightly controlled. Chelate challenge assays are a valuable guide for assessing complex stability, but as with other experimental methods such as potentiometric titrations, direct comparison of results between different experiments should be treated with caution. Finally, one should keep in mind that thermodynamic stability of a metal ion complex is only one facet that will influence the overall stability of a complex *in vivo*.

Figure 11. Structures of the various alternative ligands that have been developed for coordination of the Zr^{4+} ion and that were studied in this work. Replacements made in the calculated structures are highlighted in blue.

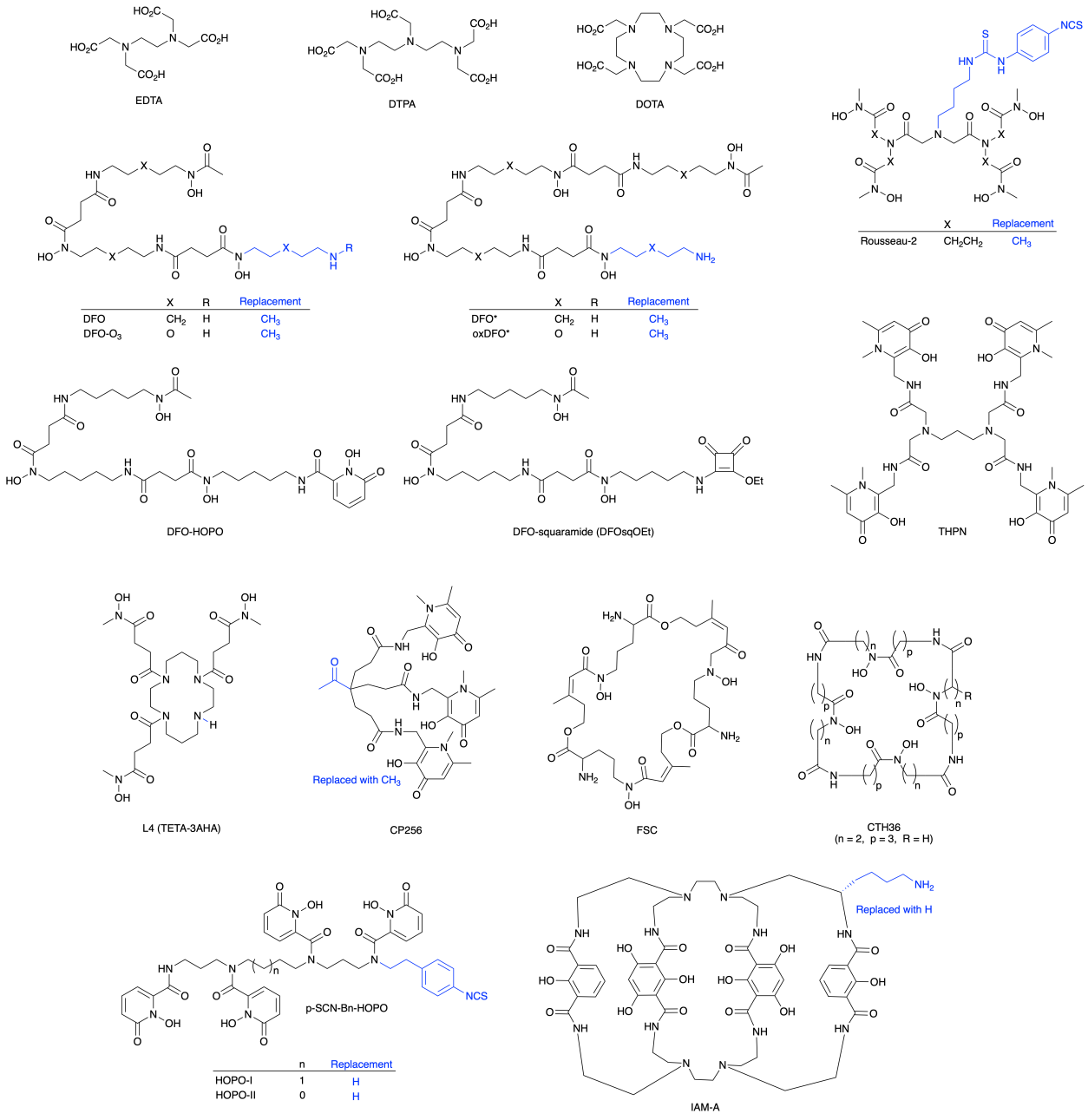

Figure 12. DFT optimised structures of 23 different Zr^{4+} complexes.

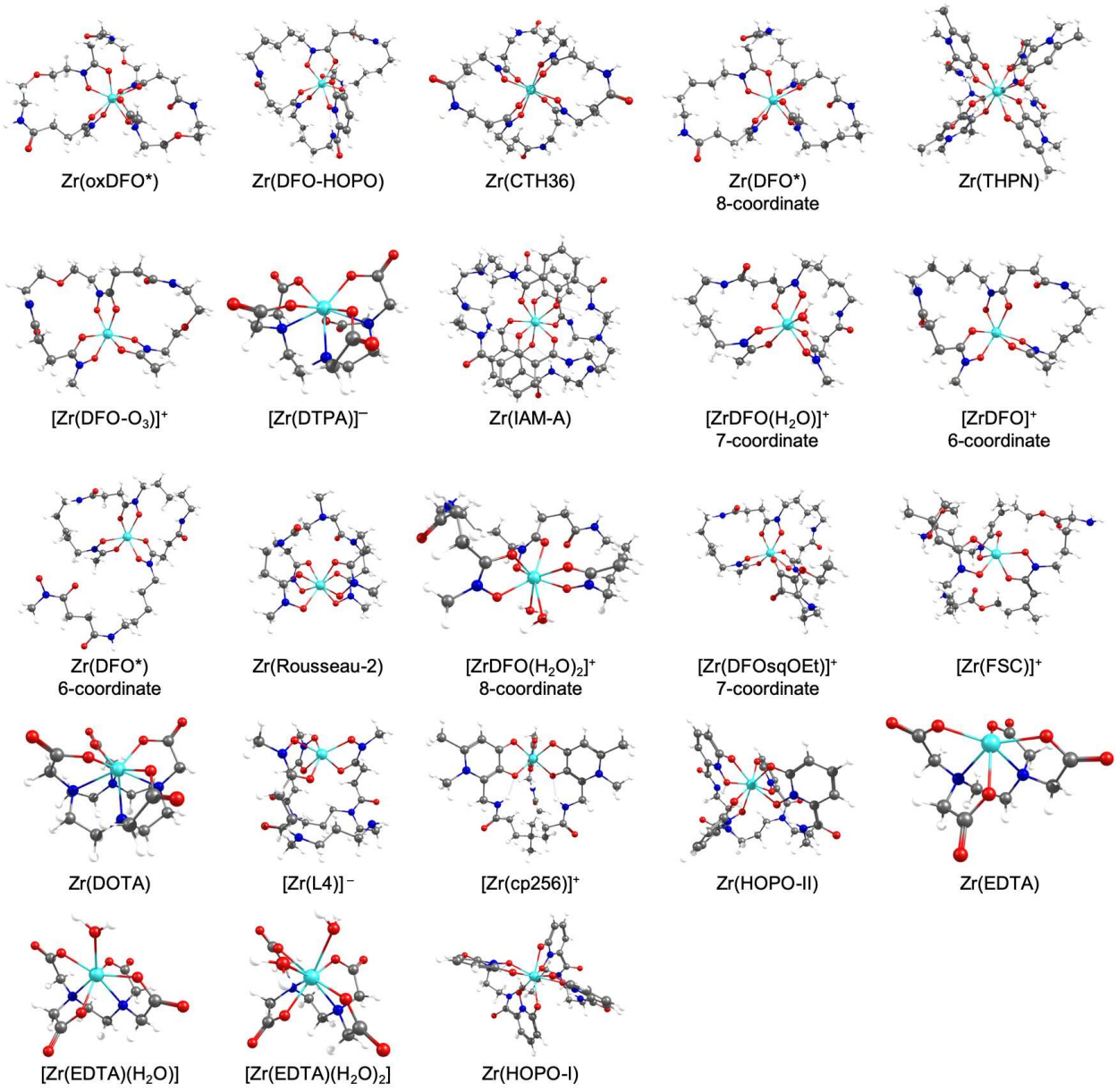

Table 2. Calculated reaction energetics for the formation of 23 Zr^{4+} complexes with different ligands. Values are computed in accordance with Equation 3 and the estimated log β values are derived from Equation 4. The relative rank order of complex stability (from highest to lowest) is also given.

B3LYP/DGDZVP/PCM	Calculated thermodynamics of complex formation (T = 298.15 K)								Reference
Complex	Δε(SCF) / kJ mol^{-1}	ΔZPE / kJ mol^{-1}	ΔG / kJ mol^{-1}	ΔH / kJ mol^{-1}	ΔS / J K^{-1} mol^{-1}	Calculated pseudo log β′	Estimated log β	Stability Rank	
Zr(EDTA)	-549.0	5.5	-611.9	-546.6	218.9	107.19	31.09	20	Friend *et al.*[56]
[ZrEDTA(H_2O)]	-551.4	4.5	-610.3	-548.0	208.9	106.91	30.95	21	
[ZrEDTA(H_2O)$_2$]	-528.0	0.1	-593.0	-520.9	241.8	103.87	29.42	22	Intorre *et al.*[66]
[ZrDFO]$^{+}$ [a] 6-coordinate	-679.3	9.4	-726.5	-677.9	162.9	127.26	41.20	10	This work
[ZrDFO(H_2O)]$^{+}$ 7-coordinate	-684.0	9.1	-730.0	-681.6	162.3	127.87	41.51	9	Racow *et al.*[57] and this work
[ZrDFO(H_2O)$_2$]$^{+}$ 8-coordinate	-670.1	11.3	-711.7	-668.4	145.2	124.67	39.89	13	Holland *et al.*[2] and this work
[Zr(DTPA)]$^{-}$	-702.7	11.6	-749.9	-703.9	154.3	131.37	43.27	7	Friend *et al.*[56]
Zr(DOTA)	-639.9	13.6	-698.8	-638.4	202.7	122.41	38.76	16	Pandya *et al.*[58]
[Zr(L4)]$^{-}$	-624.4	9.4	-669.5	-625.3	148.2	117.28	36.17	17	Boros *et al.*[59]
Zr(DFO*) 6-coordinate	-668.2	5.4	-717.1	-665.0	175.0	125.62	40.37	11	Patra *et al.*[60]
Zr(DFO*) 8-coordinate	-806.5	11.6	-843.9	-806.2	126.4	147.83	51.56	4	Patra *et al.*[60]
Zr(oxDFO*) 8-coordinate	-832.1	13.0	-873.4	-832.7	136.5	152.99	54.16	1	Briand *et al.*[61]
[Zr(DFO-O_3)]$^{+}$ 6-coordinate	-688.9	5.8	-751.1	-683.9	225.4	131.57	43.37	6	Richardson-Sanchez *et al.*[62]
Zr(HOPO-I)[c]	-548.1	14.2	-581.0	-549.3	106.2	101.77	28.36	23	Deri *et al.*[46,47]

									Sturzbecher-Hoehne *et al.*[11]
Zr(HOPO-II)[d]	-578.1	13.5	-614.5	-579.0	119.0	107.64	31.31	19	Deri *et al.*[46]
Zr(DFO-HOPO)	-821.8	12.1	-866.0	-819.6	155.6	151.69	53.51	2	Allot *et al.*[48]
$[Zr(DFOsqOEt)]^+$	-663.7	11.3	-711.0	-660.0	171.0	124.55	39.83	14	Rudd *et al.*[49]
Zr(Rousseau-2)	-677.1	7.0	-714.9	-675.8	131.2	125.23	40.18	12	Rousseau *et al.*[50]
Zr(IAM-A)	-660.2	15.9	-740.6	-643.3	326.6	129.74	42.45	8	Bhatt *et al.*[51]
Zr(THPN)[b]	-752.7	10.3	-795.4	-753.1	141.9	139.34	47.28	5	Buchwalder *et al.*[10,38]
$[Zr(FSC)]^+$	-643.5	6.6	-700.6	-640.9	200.6	122.73	38.92	15	Zhai *et al.*[52,53]
$[Zr(cp256)]^+$	-623.5	3.2	-664.5	-624.3	134.8	116.40	35.73	18	Ma *et al.*[54]
Zr(CTH36)	-791.6	8.1	-858.4	-784.9	264.8	150.37	52.84	3	Seibold *et al.*[55]

[a] The reported experimental formation constant for [ZrDFO] is log β = 40.04.[8] [b] The reported experimental formation constant for ZrTHPN is log β = 50.3(1).[10] [c] Note HOPO-I is also known as 3,4,3-LI(1,2-HOPO). [d] ZrHOPO-II is a hypothetical complex that has yet to be synthesized (personal communication Prof. Lynn Francesconi) but calculations were report.[46]

Figure 13. Plot of the estimated formation constants for 23 different Zr^{4+} complexes. Ligands derived from desferrioxamine B are shown in the right panel and alternative chelates are grouped in the left panel.

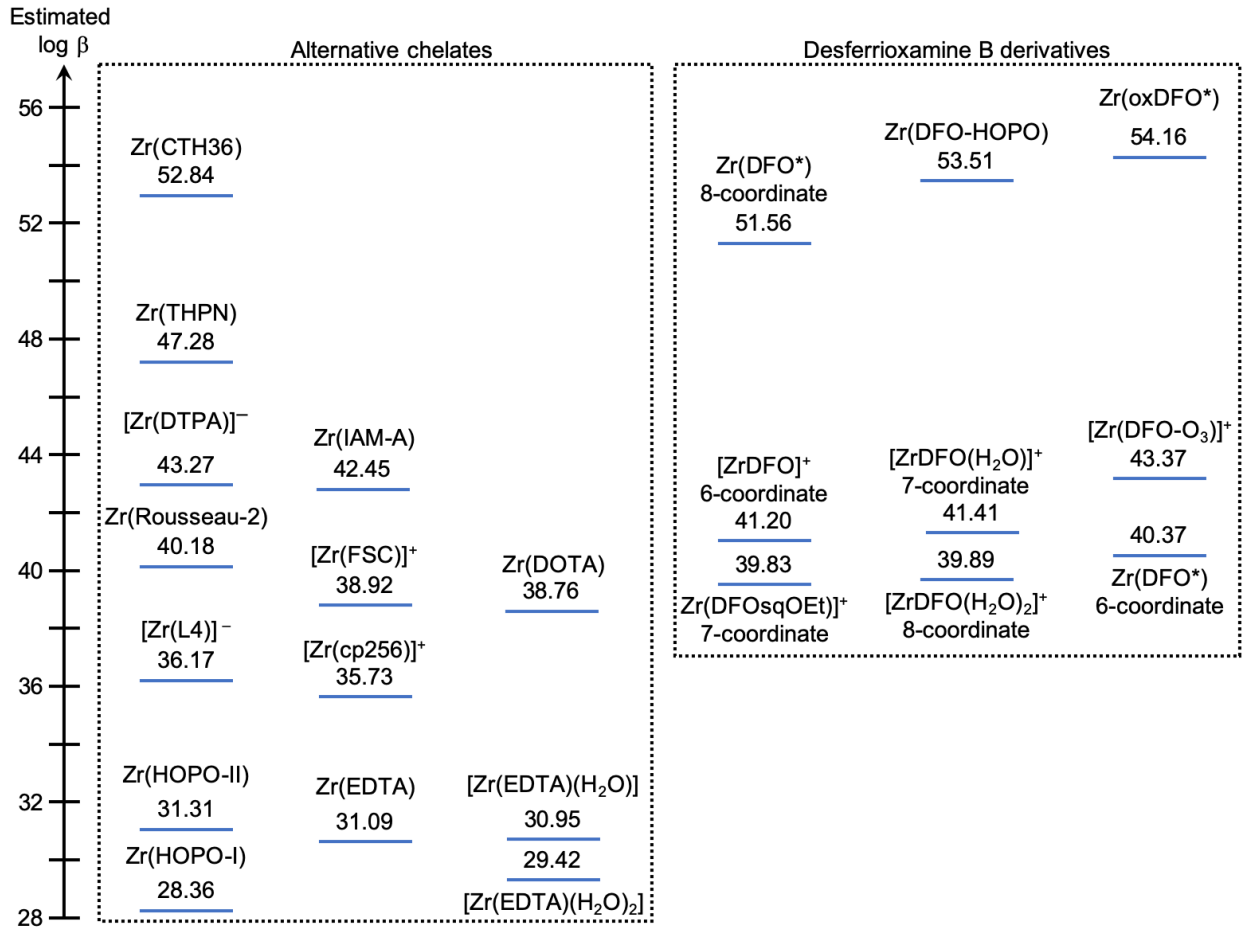

Conclusions

By considering the reaction of a free ligand with a metal-aquo ion, with appropriate treatment of the solvation models and resulting water clusters, a computational model was developed that allows for predicting of both absolute and relative formation constants for Zr^{4+} coordination compounds. DFT calculations on the various geometric isomers of Zr^{4+} in complex with the DFO ligand revealed the potential for extensive structural isomerism in solution phase. Furthermore, explicit solvation of ZrDFO with either one or two coordinated water molecules found that, in contrast to previous computational work, the 7-coordinate $[ZrDFO(H_2O)]^+$ species with a *N*-*cis*-*cis* orientation of the hydroxamate donors is likely to be the most stable species in solution. Full geometry optimisation of 23 different Zr^{4+} complexes using many of the latest ligands, and subsequent estimates of the formation constants allowed for the direct comparison of calculated thermodynamic stability of different complexes. The results provide new insight into the design of new chelates for the selective complexation of Zr^{4+} with high formation constants. The computation approach introduced here can be readily adapted to other known metal-ligand complexes, and can also be used as a tool for evaluating the potential of new ligands, prior to embarking on their synthesis.

Conflicts of interest

There are no conflicts to declare.

Acknowledgements

JPH thanks the Swiss National Science Foundation (SNSF Professorship PP00P2_163683 and PP00P2_190093), the Swiss Cancer League (Krebsliga Schweiz; KLS-4257-08-2017), and the

University of Zurich (UZH) for financial support. This project has received funding from the European Union's Horizon 2020 research and innovation programme / from the European Research Council under the Grant Agreement No 676904, ERC-StG-2015, NanoSCAN. Thanks also to Dr Amaury Guillou for helpful discussions and for proof-reading the manuscript.

Supporting Information

The Supporting Information is available free of charge on the ACS Publications website at DOI: Additional computational results and Cartesian coordinates as presented.

References

(1) Holland, J. P.; Williamson, M. J.; Lewis, J. S. Unconventional Nuclides for Radiopharmaceuticals. *Mol. Imaging* **2010**, *9* (1), 1–20.

(2) Holland, J. P.; Divilov, V.; Bander, N. H.; Smith-Jones, P. M.; Larson, S. M.; Lewis, J. S. 89Zr-DFO-J591 for ImmunoPET Imaging of Prostate-Specific Membrane Antigen (PSMA) Expression in Vivo. *J Nucl Med* **2010**, *51* (8), 1293–1300.

(3) Holland, J. P.; Vasdev, N. Charting the Mechanism and Reactivity of Zirconium Oxalate with Hydroxamate Ligands Using Density Functional Theory: Implications in New Chelate Design. *Dalt. Trans.* **2014**, *43* (26), 9872–9884.

(4) Dilworth, J. R.; Pascu, S. I. The Chemistry of PET Imaging with Zirconium-89. *Chem. Soc. Rev.* **2018**, *47* (8), 2554–2571.

(5) Fischer, G.; Seibold, U.; Schirrmacher, R.; Wängler, B.; Wängler, C. 89Zr, a Radiometal Nuclide with High Potential for Molecular Imaging with Pet: Chemistry, Applications and Remaining Challenges. *Molecules* **2013**, *18* (6), 6469–6490.

(6) Bhatt, N. B.; Pandya, D. N.; Wadas, T. J. Recent Advances in Zirconium-89 Chelator Development. *Molecules* **2018**, *23*, 638.

(7) Heskamp, S.; Raavé, R.; Boerman, O.; Rijpkema, M.; Goncalves, V.; Denat, F. 89Zr-Immuno-Positron Emission Tomography in Oncology: State-of-the-Art 89Zr Radiochemistry. *Bioconjug. Chem.* **2017**, *28* (9), 2211–2223.

(8) Toporivska, Y.; Gumienna-Kontecka, E. The Solution Thermodynamic Stability of Desferrioxamine B (DFO) with Zr(IV). *J. Inorg. Biochem.* **2019**, *198*, 110753.

(9) Savastano, M.; Bazzicalupi, C.; Ferraro, G.; Fratini, E.; Gratteri, P.; Bianchi, A. Tales of the Unexpected: The Case of Zirconium(IV) Complexes with Desferrioxamine. *Molecules*

2019, *24* (11), 2–9.

(10) Buchwalder, C.; de Guadalupe Jaraquemada-Pelaez, M.; Rousseau, J.; Merkens, H.; Rodríguez-Rodríguez, C.; Orvig, C.; Bernard, F.; Schaffer, P.; Saatchi, K.; Häfeli, U. O. Evaluation of the Tetrakis(3-Hydroxy-4-Pyridinone) Ligand THPN with Zirconium(IV): Thermodynamic Solution Studies, Bifunctionalization, and in Vivo Assessment of Macromolecular 89Zr- THPN-Conjugates. *Inorg. Chem.* **2019**, *58*, 14667–14681.

(11) Sturzbecher-Hoehne, M.; Choi, T. A.; Abergel, R. J. Hydroxypyridinonate Complex Stability of Group (IV) Metals and Tetravalent f-Block Elements: The Key to the next Generation of Chelating Agents for Radiopharmaceuticals. *Inorg. Chem.* **2015**, *54* (7), 3462–3468.

(12) Guérard, F.; Beyler, M.; Lee, Y. S.; Tripier, R.; Gestin, J. F.; Brechbiel, M. W. Investigation of the Complexation OfnatZr(Iv) And89Zr(Iv) by Hydroxypyridinones for the Development of Chelators for PET Imaging Applications. *Dalt. Trans.* **2017**, *46* (14), 4749–4758.

(13) Hancock, R. D.; Bartolotti, L. J. Prediction of Formation Constants of Metal – Ammonia Complexes in Aqueous Solution Using Density Functional Theory Calculations. **2004**, *6*, 534–535.

(14) Gutten, O.; Rulíšek, L. Predicting the Stability Constants of Metal-Ion Complexes from First Principles. *Inorg. Chem.* **2013**, *52* (18), 10347–10355.

(15) Holland, J. P.; Green, J. C.; Dilworth, J. R. Probing the Mechanism of Hypoxia Selectivity of Copper Bis(Thiosemicarbazonato) Complexes: DFT Calculation of Redox Potentials and Absolute Acidities in Solution. *Dalt. Trans.* **2006**, *6*, 783–794.

(16) Casasnovas, R.; Ortega-Castro, J.; Donoso, J.; Frau, J.; Munoz, F. Theoretical

Calculations of Stability Constants and PKa Values of Metal Complexes in Solution: Application to Pyridoxamine–Copper(II) Complexes and Their Biological Implications in AGE Inhibition†. *Phys. Chem. Chem. Phys.* **2013**, *15*, 16303–16313.

(17) Tomasi, J.; Mennucci, B.; Cammi, R. Quantum Mechanical Continuum Solvation Models. *Chem. Rev.* **2005**, *105* (8), 2999–3093.

(18) Chen, J. L.; Noodleman, L.; Case, D. A.; Bashford, D. Incorporating Solvation Effects into Density Functional Electronic Structure Calculations. *J. Phys. Chem.* **1994**, *98* (43), 11059–11068.

(19) Connolly, M. L. Solvent-Accessible Surfaces of Proteins and Nucleic Ac Ids. *Science (80-.).* **1983**, *221* (4612), 709–714.

(20) Lee, C.; Yang, W.; Parr, R. G. Development of the Colle-Salvetti Correlation-Energy Formula into a Functional of the Electron Density. *Phys. Rev. B* **1988**, *37* (2), 785–789.

(21) Becke, A. D. Density-Fnnctional Exchange-Energy Approximation with Correct Asymptotic Behavior. *Phys Rev A* **1988**, *38* (6), 3098–3100.

(22) Stephens, P. J.; Devlin, F. J.; Chabalowski, C. F.; Frisch, M. J. Ab Initio Calculation of Vibrational Absorption and Circular Dichroism Spectra Using Density Functional Force Fields. *J. Phys. Chem.* **1994**, *98* (45), 11623–11627.

(23) Godbout, N.; Salahub, D. R.; Andzelm, J.; Wimmer, E. Optimization of Gaussian-Type Basis Sets for Local Spin Density Functional Calculations. Part I. Boron through Neon, Optimization Technique and Validation. *Can. J. Chem.* **1992**, *70* (2), 560–571.

(24) Sosa, C.; Andzelm, J.; Elkin, B. C.; Wimmer, E.; Dobbs, K. D.; Dixon, D. A. A Local Density Functional Study of the Structure and Vibrational Frequencies of Molecular Transition-Metal Compounds. *J. Phys. Chem.* **1992**, *96* (16), 6630–6636.

(25) Maheshwary, S.; Patel, N.; Sathyamurthy, N.; Kulkarni, A. D.; Gadre, S. R. Structure and Stability of Water Clusters (H2O)n, n = 8-20: An Ab Initio Investigation. *J. Phys. Chem. A* **2001**, *105*, 10525–10537.

(26) Anacker, T.; Friedrich, J. New Accurate Benchmark Energies for Large Water Clusters : DFT Is Better Than Expected. *J. Comput. Chem.* **2014**, *35*, 634–643.

(27) Holmes, J. D.; Otero-de-la-roza, A.; Dilabio, G. A. Accurate Modeling of Water Clusters with Density-Functional Theory Using Atom-Centered Potentials. *J. Chem. Theory Comput.* **2017**, *13*, 4205−4215.

(28) Hartmann, M.; Clark, T.; Van Eldik, R. Hydration and Water Exchange of Zinc(II) Ions. Application of Density Functional Theory. *J. Am. Chem. Soc.* **1997**, *119* (33), 7843–7850.

(29) Markham, G. D.; Glusker, J. P.; Bock, C. W. The Arrangement of First- and Second-Sphere Water Molecules in Divalent Magnesium Complexes: Results from Molecular Orbital and Density Functional Theory and from Structural Crystallography. *J. Phys. Chem. B* **2002**, *106* (19), 5118–5134.

(30) Bock, C. W.; Markham, G. D.; Katz, A. K.; Glusker, J. P. The Arrangement of First- and Second-Shell Water Molecules in Trivalent Aluminum Complexes: Results from Density Functional Theory and Structural Crystallography. *Inorg. Chem.* **2003**, *42* (5), 1538–1548.

(31) Beret, E. C.; Galbis, E.; Pappalardo, R. R.; Sánchez Marcos, E. Opposite Effects of Successive Hydration Shells on the Aqua Ion Structure of Metal Cations. *Mol. Simul.* **2009**, *35* (12–13), 1007–1014.

(32) Yoo, S.; Apra, E.; Zeng, X. C.; Xantheas, S. S. High-Level Ab Initio Electronic Structure Calculations OfWater Clusters (H2O)16 and (H2O)17: A New Global Minimum for (H2O)16 Soohaeng. *J. Phys. Chem. Lett.* **2010**, *1*, 3122–3127.

(33) Medvedev, M. G.; Bushmarinov, I. S.; Sun, J.; Perdew, J. P.; Lyssenko, K. A. Density Functional Theory Is Straying from the Path toward the Exact Functional. *Science (80-.).* **2017**, *355* (6320), 49–52.

(34) Bryantsev, V. S.; Diallo, M. S.; Goddard, W. A. Computational Study of Copper(II) Complexation and Hydrolysis in Aqueous Solutions Using Mixed Cluster/Continuum Models. *J. Phys. Chem. A* **2009**, *113* (34), 9559–9567.

(35) Burda, J. V.; Pavelka, M.; Šimánek, M. Theoretical Model of Copper Cu(I)/Cu(II) Hydration. DFT and Ab Initio Quantum Chemical Study. *J. Mol. Struct. THEOCHEM* **2004**, *683* (1–3), 183–193.

(36) Dhungana, S.; White, P. S.; Crumbliss, A. L. Crystal Structure of Ferrioxamine B: A Comparative Analysis and Implications for Molecular Recognition. *J. Biol. Inorg. Chem.* **2001**, *6* (8), 810–818.

(37) Borgias, B.; Hugi, A. D.; Raymond, K. N. Isomerization and Solution Structures of Desferrioxamine B Complexes of Al3+and Ga3+1. *Inorg. Chem.* **1989**, *28* (18), 3538–3545.

(38) Buchwalder, C.; Rodríguez-Rodríguez, C.; Schaffer, P.; Karagiozov, S. K.; Saatchi, K.; Häfeli, U. O. A New Tetrapodal 3-Hydroxy-4-Pyridinone Ligand for Complexation Of89zirconium for Positron Emission Tomography (PET) Imaging. *Dalt. Trans.* **2017**, *46* (29), 9654–9663.

(39) Schwarzenbach, G.; Schwarzenbach, K. Die Stabilitat Der Eisen(II1)-Komplexe Einfacher Hydroxamsauren Und Des Ferrioxamins B. *Helv. Chim. Acta* **1963**, *22* (1902), 1390–1400.

(40) Anderegg, G.; L'Eplattenier, F.; Schwarzenbach, G. Hydroxamatkomplexe II. Die

Anwendung Der PH-Methode. *Helv. Chim. Acta* **1963**, *46* (4), 1400–1408.

(41) Evers, A.; Hancock, R. D.; Martell, A. E.; Motekaitis, R. J. Metal Ion Recognition in Ligands with Negatively Charged Oxygen Donor Groups . Complexation of Fe(III), Ga(III), In(III), Al(III), and Other Highly Charged Metal Ions. *Inorg. Chem.* **1989**, *27* (9), 2189–2195.

(42) Zu, D. L.; Hider, R. C. Design of Iron Chelators with Therapeutic Application. *Coord. Chem. Rev.* **2002**, *232* (2002), 151–171.

(43) Kruft, B. I.; Harrington, J. M.; Duckworth, O. W.; Jarzęcki, A. A. Quantum Mechanical Investigation of Aqueous Desferrioxamine B Metal Complexes: Trends in Structure, Binding, and Infrared Spectroscopy. *J. Inorg. Biochem.* **2013**, *129*, 150–161.

(44) Hernlem, B. J.; Vane, L. M.; Sayles, G. D. Stability Constants for Complexes of the Siderophore Desferrioxamine B with Selected Heavy Metal Cations. *Inorganica Chim. Acta* **1996**, *244*, 179–184.

(45) Duckworth, O. W.; Bargar, J. R.; Jarzecki, A. A.; Oyerinde, O.; Spiro, T. G.; Sposito, G. The Exceptionally Stable Cobalt(III)-Desferrioxamine B Complex. *Mar. Chem.* **2009**, *113* (1–2), 114–122.

(46) Deri, M. A.; Ponnala, S.; Zeglis, B. M.; Pohl, G.; Dannenberg, J. J.; Lewis, J. S.; Francesconi, L. C. Alternative Chelator for 89Zr Radiopharmaceuticals: Radiolabeling and Evaluation of 3,4,3-(LI-1,2-HOPO). *J. Med. Chem.* **2014**, *57* (11), 4849–4860.

(47) Deri, M. A.; Ponnala, S.; Kozlowski, P.; Burton-Pye, B. P.; Cicek, H. T.; Hu, C.; Lewis, J. S.; Francesconi, L. C. P-SCN-Bn-HOPO: A Superior Bifunctional Chelator for 89Zr ImmunoPET. *Bioconjug. Chem.* **2015**, *26* (12), 2579–2591.

(48) Allott, L.; Da Pieve, C.; Meyers, J.; Spinks, T.; Ciobota, D. M.; Kramer-Marek, G.; Smith,

G. Evaluation of DFO-HOPO as an Octadentate Chelator for Zirconium-89. *Chem. Commun.* **2017**, *53* (61), 8529–8532.

(49) Rudd, S. E.; Roselt, P.; Cullinane, C.; Hicks, R. J.; Donnelly, P. S. A Desferrioxamine B Squaramide Ester for the Incorporation of Zirconium-89 into Antibodies. *Chem. Commun.* **2016**, *52* (80), 11889–11892.

(50) Rousseau, J.; Zhang, Z.; Dias, G. M.; Zhang, C.; Colpo, N.; Bénard, F.; Lin, K. S. Design, Synthesis and Evaluation of Novel Bifunctional Tetrahydroxamate Chelators for PET Imaging of 89Zr-Labeled Antibodies. *Bioorganic Med. Chem. Lett.* **2017**, *27* (4), 708–712.

(51) Bhatt, N. B.; Pandya, D. N.; Xu, J.; Tatum, D.; Magda, D.; Wadas, T. J. Evaluation of Macrocyclic Hydroxyisophthalamide Ligands as Chelators for Zirconium-89. *PLoS One* **2017**, *12* (6), 1–13.

(52) Zhai, C.; Summer, D.; Rangger, C.; Franssen, G. M.; Laverman, P.; Haas, H.; Petrik, M.; Haubner, R.; Decristoforo, C. Novel Bifunctional Cyclic Chelator for ^{89}Zr Labeling-Radiolabeling and Targeting Properties of RGD Conjugates. *Mol. Pharm.* **2015**, *12* (6), 2142–2150.

(53) Zhai, C.; He, S.; Ye, Y.; Rangger, C.; Kaeopookum, P.; Summer, D.; Haas, H.; Kremser, L.; Lindner, H.; Foster, J.; Sosabowski, J.; Decristoforo. Rational Design, Synthesis and Preliminary Evaluation of Novel Fusarinine C-Based Chelators for Radiolabeling with Zirconium-89. *Biomolecules* **2019**, *9* (3), 91.

(54) Ma, M. T.; Meszaros, L. K.; Paterson, B. M.; Berry, D. J.; Cooper, M. S.; Ma, Y.; Hider, R. C.; Blower, P. J. Tripodal Tris(Hydroxypyridinone) Ligands for Immunoconjugate PET Imaging with ^{89} Zr $^{4+}$: Comparison with Desferrioxamine-B. *Dalt. Trans.* **2015**, *44* (11),

4884–4900.

(55) Seibold, U.; Wängler, B.; Wängler, C. Rational Design, Development, and Stability Assessment of a Macrocyclic Four-Hydroxamate-Bearing Bifunctional Chelating Agent for 89Zr. *ChemMedChem* **2017**, *12* (18), 1555–1571.

(56) Friend, M. T.; Wall, N. A. Stability Constants for Zirconium(IV) Complexes with EDTA, CDTA, and DTPA in Perchloric Acid Solutions. *Inorganica Chim. Acta* **2019**, *484* (September 2018), 357–367.

(57) Racow, E. E.; Kreinbihl, J. J.; Cosby, A. G.; Yang, Y.; Pandey, A.; Boros, E.; Johnson, C. J. A General Approach to Direct Measurement of the Hydration State of Coordination Complexes in the Gas Phase : Variable Temperature Mass Spectrometry A General Approach to Direct Measurement of the Hydration State of Coordination Complexes in the Gas Phase. *J. Am. Chem. Soc.* **2019**, *147* (37), 14650–14660.

(58) Pandya, D. N.; Bhatt, N.; Yuan, H.; Day, C. S.; Ehrmann, B. M.; Wright, M.; Bierbach, U.; Wadas, T. J. Zirconium Tetraazamacrocycle Complexes Display Extraordinary Stability and Provide a New Strategy for Zirconium-89-Based Radiopharmaceutical Development. *Chem. Sci.* **2017**, *8* (3), 2309–2314.

(59) Boros, E.; Holland, J. P.; Kenton, N.; Rotile, N.; Caravan, P. Macrocycle-Based Hydroxamate Ligands for Complexation and Immunoconjugation of 89Zirconium for Positron Emission Tomography (PET) Imaging. *Chempluschem* **2016**, *81* (3), 274–281.

(60) Patra, M.; Bauman, A.; Mari, C.; Fischer, C. A.; Blacque, O.; Häussinger, D.; Gasser, G.; Mindt, T. L. An Octadentate Bifunctional Chelating Agent for the Development of Stable Zirconium-89 Based Molecular Imaging Probes. *Chem. Commun.* **2014**, *50* (78), 11523–11525.

(61) Briand, M.; Aulsebrook, M. L.; Mindt, T. L.; Gasser, G. A Solid Phase-Assisted Approach for the Facile Synthesis of a Highly Water-Soluble Zirconium-89 Chelator for Radiopharmaceutical Development. *Dalt. Trans.* **2017**, *46* (47), 16387–16389.

(62) Richardson-Sanchez, T.; Tieu, W.; Gotsbacher, M. P.; Telfer, T. J.; Codd, R. Exploiting the Biosynthetic Machinery of: Streptomyces Pilosus to Engineer a Water-Soluble Zirconium(IV) Chelator. *Org. Biomol. Chem.* **2017**, *15* (27), 5719–5730.

(63) Guérard, F.; Lee, Y. S.; Tripier, R.; Szajek, L. P.; Deschamps, J. R.; Brechbiel, M. W. Investigation of Zr(Iv) and 89Zr(Iv) Complexation with Hydroxamates: Progress towards Designing a Better Chelator than Desferrioxamine B for Immuno-PET Imaging. *Chem. Commun.* **2013**, *49* (10), 1002–1004.

(64) Guérard, F.; Lee, Y. S.; Brechbiel, M. W. Rational Design, Synthesis, and Evaluation of Tetrahydroxamic Acid Chelators for Stable Complexation of Zirconium(IV). *Chem. - A Eur. J.* **2014**, *20* (19), 5584–5591.

(65) Brown, C. J. M.; Gotsbacher, M. P.; Holland, J. P.; Codd, R. Endo -Hydroxamic Acid Monomers for the Assembly of a Suite of Non-Native Dimeric Macrocyclic Siderophores Using Metal-Templated Synthesis . *Inorg. Chem.* **2019**, *58*, 13591–13603.

(66) Intorre, B. I.; Martell, A. E. Zirconium Complexes in Aqueous Solution. I. Reaction with Multidentate Ligands. *J. Am. Chem. Soc.* **1960**, *82* (2), 358–364.

TOC Graphic

A simple computational approach is developed to predict the absolute and relative thermodynamic stabilities of zirconium complexes. The model is used to evaluate the characteristics of 23 different complexes that have been designed for potential use in radiopharmaceutical synthesis.